

# Lefschetz-thimble inspired analysis of the Dykhne-Davis-Pechukas method and an application for the Schwinger Mechanism

Kenji Fukushima<sup>a,b</sup>, Takuya Shimazaki<sup>a</sup>

<sup>a</sup>*Department of Physics, The University of Tokyo, 7-3-1 Hongo, Bunkyo-ku, Tokyo 113-0033, Japan*

<sup>b</sup>*Institute for Physics of Intelligence (IPI), The University of Tokyo, 7-3-1 Hongo, Bunkyo-ku, Tokyo 113-0033, Japan*

---

## Abstract

Dykhne-Davis-Pechukas (DDP) method is a common approximation scheme for the transition probability in two-level quantum systems, as realized in the Landau-Zener effect, leading to an exponentially damping form comparable to the Schwinger pair production rate. We analyze the foundation of the DDP method using a modern complex technique inspired by the Lefschetz-thimble method. We derive an alternative and more adaptive formula that is useful even when the DDP method is inapplicable. As a benchmark, we study the modified Landau-Zener model and compare results from the DDP and our methods. We then revisit a derivation of the Schwinger Mechanism of particle production under electric fields using the DDP and our methods. We find that the DDP method gets worse for the Sauter type of short-lived electric pulse, while our method is still a reasonable approximation. We also study the Dynamically Assisted Schwinger Mechanism in two methods.

*Keywords:* Schwinger Mechanism, Complex analysis, Dykhne-Davis-Pechukas method, Two-level quantum systems

---

## 1. Introduction

Nonadiabatic transitions are ubiquitous phenomena in physics problems such as dielectric breakdown of a Mott insulator [1, 2], shortcuts to adiabaticity in quantum manipulation [3, 4], population transfer in optics [5–8], and so on. In many-body systems theoretical treatments often reduce to one-quasi-particle problem on energy levels formed by surrounding mean fields as exemplified in the band theory of solids, the shell model of nuclei, etc. Then, the essence of quantum tunneling phenomena is in effect modeled in a form of relatively simple system in Quantum Mechanics. In many-body systems of Quantum Field Theories nonadiabatic transitions from an anti-particle (negative energy) state to a particle (positive energy) state can be interpreted as pair particle production, which is actually what we will address in details in this paper. Several examples are found in the Schwinger Mechanism [9–11] (see Refs. [12, 13] for reviews), i.e., pair production under external electric field, and also in high-energy nuclear collision where particle

---

*Email addresses:* fuku@nt.phys.s.u-tokyo.ac.jp (Kenji Fukushima),  
shimazaki@nt.phys.s.u-tokyo.ac.jp (Takuya Shimazaki)

*Preprint submitted to Elsevier*

*November 12, 2019*

production occurs from strong chromo-electromagnetic fields. As long as spatial inhomogeneity is assumed for such problems, we can compute the transition rate for each momentum mode in the same way as two-level systems in Quantum Mechanics. Similarly, the Hawking radiation can be also treated as a simple Quantum Mechanical problem [14]. It is thus an important theoretical challenge, not closed to Quantum Mechanics but relevant generally to Quantum Field Theories, to consider handy and multi-purpose formulas for estimating quantum transition amplitudes.

To attack this challenge there are various approaches, and here, let us pick up one specific method called the Dykhne-Davis Pechukas (DDP) method, which is of frequent choice particularly in condensed matter physics fields (see, Refs. [1, 2] for example). In the early 1930's pioneering works paved a way for real-time quantum dynamics beyond the adiabatic theorem. Among them, Landau and Zener especially derived an analytical formula for the transition probability in a simple two-level quantum model which is known as the Landau-Zener model today [15, 16]. Dykhne proposed an approximation method with complexified time in such a way adaptive for more general two-level quantum systems [17]. Davis and Pechukas derived the method in a clearer manner removing ad hoc assumptions in Dykhne's formulation [18], so the DDP method aka the Landau-Dykhne method was named after these founders.

There are many preceding literatures on the DDP method; examples include the adiabatic limit [19], nonlinear level-crossing models [20], nonadiabatic transitions in multi-level systems [21], and so on. We note that more references are easily found for what is called the Landau-Zener formula, but the DDP method is a more sophisticated formulation than the Landau-Zener formula. The most non-trivial is the fact that the DDP method mystically reproduces the exact analytical result for the Landau-Zener model, although the derivation of the DDP method involves several approximating steps as we will explain later.

Apart from technical details, at this point, we would remark that the validity of the DDP method requires the following assumptions: (1) The difference of two-level adiabatic energies  $\delta E(t)$  has a closing point  $t_c \notin \mathbb{R}$  in complex- $t$  plane where  $\delta E(t_c) = 0$  is satisfied. (2) The  $t$ -contour can be deformed from the real axis to the DDP choice (which will be specified later) without hitting any poles in complex- $t$  plane. When these assumptions hold, it is empirically known that the DDP method is a good approximation, while there are a few exceptions due to pathological behavior of  $\delta E(t \sim \pm\infty)$  [22, 23]. In the present work we will pay our special attention on a model which violates the condition (2) as mentioned above. As soon as poles hinder the deformation of the integration contour, the DDP method breaks down and we must employ a more firm method taking proper account of the complex structures.

The aim of the present work is to establish another approximate method based on the Lefschetz-thimble method. The Lefschetz-thimble method is a modern complex analysis treating an integral with complexified variables. The original targets of the Lefschetz-thimble method were path integrals in quantum mechanics [24], quantum gravity [25], and quantum field theory. Some examples for recent applications are found for the QCD sign problem at finite density [26–28] (which is investigated also in a more idealized one-site fermion model [29]), the real-time Feynman path integral [30, 31], the false vacuum decay [32], and so on. This method provides us with a clear prescription for complex saddle points and attached contours as well as interesting physics interpretations (see Ref. [33] for a review). The difference from standard saddle-point approximation is that, when multiple saddle points appear, this method clearly tells us which points we should take and which we should not.

In this work we develop the Lefschetz-thimble inspired method to calculate the transition probability in two-level quantum systems. Our approach based on the Lefschetz-thimble method has advantages over the conventional DDP method. First of all, our method is an approximation

under theoretical control and can be improved systematically. Sometimes the DDP method works artificially better beyond the approximation limit as we discuss later. It is, however, hard to judge how reliable the DDP method is, *a priori*, in general. Second, our method is not prevented by poles that obstruct the DDP method. Therefore, the applicability of our method is much wider than the DDP method. We explicitly demonstrate the above advantages using the modified Landau-Zener model as a warm-up exercise.

Armed with experiences of such concrete examples, we shall proceed to another related problem of the Schwinger Mechanism. Although the Schwinger Mechanism at finite temperature is an active research field lately [34–37], we limit ourselves to the exponent only of the production rate at zero temperature, and will not calculate the prefactor in this paper, for simplicity. We can show that the DDP method immediately leads to the famous Schwinger exponential factor correctly for constant electric field. We next consider a little more non-trivial case with pulsed electric field in a Sauter-type form. We see that the complex structures are a little more complicated, but for a pulse whose scale is smaller than the mass gap, we can still utilize the DDP method to obtain the correct estimate. Interestingly, for a sharp pulse, on the other hand, the estimate from the DDP method gets worse. Finally, we will consider a combination of a pulse on top of constant electric field. In this case the exponent is significantly suppressed for particular parameter regions, and this suppression mechanism is commonly referred to as the Dynamically Assisted Schwinger Mechanism [38]. The Dynamically Assisted Schwinger Mechanism helps to realize experimentally the Schwinger Mechanism which has not been verified yet, so it has been actively attracting attention [39–46]. Again, the DDP method can reproduce the exponent correctly as long as the pulse is broad enough. We will make a quantitative comparison between results from the fully numerical calculation, the DDP method, and our method.

Throughout this work we adopt physical units of  $\hbar = c = 1$ .

## 2. Transition amplitude in two-level quantum systems

We consider two-level systems as the simplest quantum mechanical example. Without loss of generality, we can reduce two-level problems into the ones described by the following Hamiltonian [47],

$$H(t) = \frac{1}{2} \begin{bmatrix} \alpha(t) & V(t) \\ V(t) & -\alpha(t) \end{bmatrix}, \quad (1)$$

where  $\alpha(t)$  and  $V(t)$  are real-valued functions. We define adiabatic eigenvalues  $E_{\pm}(t)$  and adiabatic eigenstates  $|\chi_{\pm}(t)\rangle$  obtained from  $H(t)$  as

$$H(t) |\chi_{\pm}(t)\rangle = E_{\pm}(t) |\chi_{\pm}(t)\rangle. \quad (2)$$

We choose  $E_+(t) \geq E_-(t)$  for  $t \in \mathbb{R}$ . We denote a physical state by  $|\psi(t)\rangle$  that obeys the Schrödinger equation and expand  $|\psi(t)\rangle$  in terms of  $|\chi_{\pm}(t)\rangle$ , i.e.,

$$|\psi(t)\rangle = \sum_{i=\pm} a_i(t) e^{-i\mathcal{E}_i(t)} |\chi_i(t)\rangle \quad \text{with} \quad \mathcal{E}_{\pm}(t) = \int_0^t dt' E_{\pm}(t'). \quad (3)$$

We derive the equations of motion for  $a_{\pm}(t)$  from the Schrödinger equation as

$$\dot{a}_{\pm}(t) = \pm \eta(t) e^{\pm i\Delta(t)} a_{\mp}(t), \quad (4)$$

where

$$\Delta(t) = \mathcal{E}_+(t) - \mathcal{E}_-(t) = \int_0^t dt' \delta E(t'), \quad (5)$$

$$\eta(t) = \langle \chi_-(t) | \frac{d}{dt} | \chi_+(t) \rangle = \frac{1}{2} \frac{V\dot{\alpha} - \dot{V}\alpha}{\alpha^2 + V^2} \quad (6)$$

with  $\delta E(t) = E_+(t) - E_-(t) = \sqrt{\alpha(t)^2 + V(t)^2}$ . If we solve the time evolution with initial conditions,  $a_-(-\infty) = 1$  and  $a_+(-\infty) = 0$ , then  $P = |a_+(\infty)|^2$  gives the transition probability from  $|\chi_-(-\infty)\rangle$  to  $|\chi_+(\infty)\rangle$ .

To this end of obtaining  $P$ , we integrate Eq. (4) with respect to  $t$  to find,

$$a_+(\infty) = \int_{-\infty}^{\infty} dt a_-(t) \eta(t) e^{i\Delta(t)} \simeq \int_{-\infty}^{\infty} dt e^{F(t)}, \quad (7)$$

where we defined  $F(t) = i\Delta(t) + \ln \eta(t)$ . To go to the last expression we employed the first order truncation in the iterative approximation, that is, we set  $a_-(t) = 1$ . Physically speaking, the time evolution should generally involve many alternate transitions between  $|\chi_{\pm}(t)\rangle$ , but the above first order truncation corresponds to an approximation by one time transition from  $|\chi_-(t)\rangle$  to  $|\chi_+(t)\rangle$ . In other words this is the *definition* of quantity of our current interest, as is also relevant to discussions on the Schwinger Mechanism (see the difference between  $f$  and  $w$  in Sec. IIB of Ref. [48]). At this point we make clear that Eq. (7) is the starting point for further approximations including the DDP method.

### 2.1. DDP method

The DDP method is derived from Eq. (7) with deformed integration contour in terms of complexified  $t$  [18]. In what follows below, we consider the situation where there exists only one closing point,  $t_c$ , such that  $\delta E(t_c) = 0$  in upper complex- $t$  plane (see Fig. 1 for a schematic illustration). [Let us comment on generalization to multiple closing points in upper complex- $t$  plane. In such a case the DDP method prescribes that the nearest closing point(s) contributes to the amplitude with proper weights which are calculable. Our proposed approach, explicated shortly, is also applicable to the case with multiple closing points in a similar fashion.] Equivalently, this condition is translated into

$$\left. \frac{\partial \Delta}{\partial t} \right|_{t=t_c} = 0. \quad (8)$$

Here, we used a partial derivative, for in later discussions we will introduce spatial coordinates.

The second assumption in the DDP method, i.e., deformability of the integration contour, needs some more explanations. The complex- $t$  contour adopted in the DDP method is the one determined by

$$\text{Im}\Delta(t) = \text{Im}\Delta(t_c). \quad (9)$$

The second assumption holds if there are no poles between the real axis and this contour. Still, we would note that the deformability is subtle because the contour at infinity may have a non-vanishing contribution. Once these conditions for the deformability are premised, the transition amplitude from  $|\chi_-(-\infty)\rangle$  to  $|\chi_+(\infty)\rangle$  is approximated by  $a_+(\infty) \simeq e^{i\Delta(t_c)}$  so that the transition probability is

$$P \simeq e^{-2\text{Im}\Delta(t_c)}. \quad (10)$$

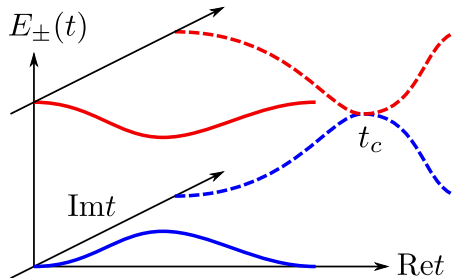


Figure 1: Schematic illustration of the closing point  $t_c$  in the complex- $t$  plane.

With the above form, the DDP choice (9) could be intuitive to some extent; only the imaginary part contributes to the exponent, and the real part represents an oscillation phase. Along the contour of Eq. (9), the stationary point approximation at  $t = t_c$  (if it corresponds to the stationary point, which is not always the case, though) finds a dominant exponential term that is Eq. (10). As we will closely discuss later, Eq. (10) is a powerful tool to investigate general transitional problems including quantum field theoretical problems such as the Schwinger Mechanism in electric fields in a particular regime.

The DDP method provides us with a fascinating interpretation for the transitional processes. Two adiabatic eigenenergies are typically gapped as illustrated in Fig. 1, and the transition needs quantum tunneling. Once the notion of time is extended to the complex plane, however, it is possible to take a *detour* to reach  $t_c$  where two states touch each other, as depicted in Fig. 1, and thus the transition can occur classically there. In some sense the idea is analogous to the instanton calculus based on classical trajectory with Euclidean time, but the current formulation is more general in the while complex- $t$  plane.

## 2.2. Complex analysis

The DDP method is certainly interesting and useful, but unfortunately, it may fail when it fails as we will see. Thus, we shall consider an independent approximation scheme here. To approximate the integral (7), instead of the DDP method, we employ the complex analysis inspired by recent developments of the Lefschetz-thimble method. One can say that the Lefschetz-thimble method is a modern refinement of the steepest descent method. We assume that saddle points,  $t_s$ , of  $F(t)$  are nondegenerate, i.e.,

$$\left. \frac{\partial F}{\partial t} \right|_{t=t_s} = \left[ i \frac{\partial \Delta}{\partial t} + \eta(t)^{-1} \frac{\partial \eta}{\partial t} \right]_{t=t_s} = 0, \quad \left. \frac{\partial^2 F}{\partial t^2} \right|_{t=t_s} = |F''(t_s)| e^{i\phi} \neq 0, \quad (11)$$

where  $0 \leq \phi < 2\pi$ . We note that the difference between  $t_c$  and  $t_s$  results from the second term in the square parentheses involving  $\eta$  [see Eq. (8)]. We expand  $F(t)$  around the saddle point,  $t_s$ , as

$$F(t) = F(t_s) + \frac{|F''(t_s)|}{2} r^2 e^{i(\phi+2\theta)} + O(r^3). \quad (12)$$

We note that we introduced the polar form,  $t - t_s = r e^{i\theta}$ . The contour along  $\phi + 2\theta = \pi$  around  $t_s$  is directed toward a steepest descent. According to the Lefschetz-thimble method, the original integration contour is decomposed into steepest descents from saddle points. The  $i$ -th saddle

point,  $t_{s,i}$ , is attached to a steepest descent  $\mathcal{J}_i$  and a steepest ascent  $\mathcal{K}_i$ . We note that  $\text{Im}F(t) = (\text{const.})$  holds on  $\mathcal{J}_i$ , which makes a sharp contrast to the previous condition (9) that keeps, apart from  $\ln \eta(t)$ ,  $\text{Re}F(t)$  constant. Now, it is a crucial process to specify which saddle points should be taken into account to recover the original integral *exactly*. It is known that  $\{\mathcal{J}_i\}$  generate the 1st relative homology  $H_1(X, X_{-\infty}, \mathbb{Z})$  when  $X$  denotes complex- $t$  plane and  $X_T$  denotes  $\{t \in X | \text{Re}F(t) < T\}$  [25]. The bases of  $H_1(X, X_{-\infty}, \mathbb{Z})$  are called the Lefschetz thimbles in the Picard-Lefschetz theory, which are nothing but steepest descents in this case. The original integration contour is the real axis denoted here by  $C_0$ . Then, the original integral is recovered exactly if the deformed contour is chosen to be

$$C = \sum_i n_i \mathcal{J}_i, \quad (13)$$

where the Morse index,  $n_i \in \mathbb{Z}$ , must be carefully determined, and the calculational prescription is well established as

$$n_i = \langle C_0, \mathcal{K}_i \rangle, \quad (14)$$

where  $\langle C_0, \mathcal{K}_i \rangle$  counts the intersection number between  $C_0$  and  $\mathcal{K}_i$  with orientation in accord with  $\langle \mathcal{J}_i, \mathcal{K}_j \rangle = \delta_{ij}$ . Here, we emphasize that Eq. (13) is the most essential difference from the standard complex analysis which simply prescribes contour deformations based on Cauchy's integral formula. One might think that complex poles would make things complicated as is the case for the DDP formula, but the appropriate choice of  $\mathcal{J}_i$  and  $n_i$  already takes care of such complications.

With Eqs. (7), (12), and (13), the saddle-point approximation leads to

$$a_+(\infty) \simeq \sum_i n_i e^{i\theta_i + F(t_{s,i})} \sqrt{\frac{2\pi}{|F''(t_{s,i})|}} \quad (15)$$

after our performing the Gaussian integration with respect to  $r$  on each  $\mathcal{J}_i$ . Here, again, we stress that the determination of  $n_i$  is crucially important in above formula (15). We will apply Eq. (15) to a two-level quantum system in order to demonstrate how this formula works more robustly than the DDP method in wider parameter regions.

### 2.3. Benchmark test in the simplest example

We note that the DDP method happens to reproduce the analytical formula exactly in a special model called the Landau-Zener model. The diabatic energies are, however, divergent unphysically as  $t \rightarrow \pm\infty$  and the interaction between diabatic states is constant in the Landau-Zener model. It is thus desirable to augment the Landau-Zener model with  $t$ -dependence so that the asymptotic behavior becomes more treatable. We consider the following Hamiltonian,

$$H(t) = \frac{\Lambda}{2\tau \sqrt{1 + (t/T)^2}} \begin{pmatrix} t/\tau & 1 \\ 1 & -t/\tau \end{pmatrix}, \quad (16)$$

where  $\Lambda$ ,  $\tau$ , and  $T$  are positive parameters. In the limit of  $T \rightarrow \infty$ , this model reduces to the Landau-Zener model. So, we call the above model defined by Eq. (16) the modified Landau-Zener model, which is sometimes called the simple Lorentzian singularity model [19]. It is easy to find the difference of adiabatic energies given by

$$\delta E(t) = \frac{T\Lambda}{\tau^2} \sqrt{\frac{t^2 + \tau^2}{t^2 + T^2}}. \quad (17)$$

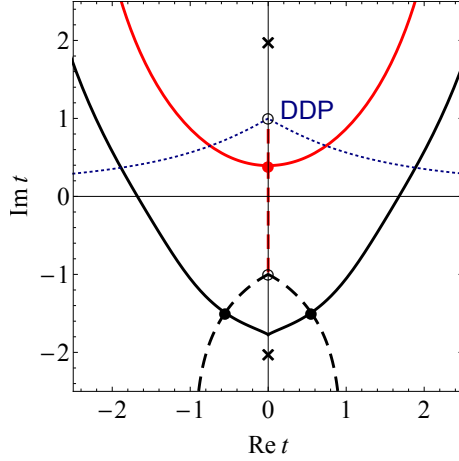


Figure 2: Analytical structure of  $F(t)$  in complex- $t$  plane in the modified Landau-Zener model with  $(T, \tau, \Lambda) = (2, 1, 1)$ . The upper (and lower) solid line represents the steepest descent with  $n = 1$  (and  $n = 0$ , respectively). The dashed lines are the steepest ascents and the dotted line is the DDP contour. The cross dots represent the poles, the open-circle dots indicate the closing points, and the filled-circle dots are the saddle points.

This expression of  $\delta E(t)$  has a closing point at  $t = i\tau$  and a pole at  $t = iT$  in upper complex- $t$  plane. For  $T > \tau$  the DDP method is applicable since we can deform the integration contour without hitting the pole. In contrast, the DDP method breaks down for  $T \leq \tau$ , while our method based on Eq. (15) works for any  $T$  and  $\tau$ .

### 2.3.1. When the DDP method succeeds

For  $T > \tau$  where the DDP method works, we shall quantitatively justify our proposed method compared with the DDP method. The transition probability from the DDP method of Eq. (10) is given by

$$P \simeq \exp \left[ -\frac{2T\Lambda}{\tau} E \left( \frac{\tau}{T}, \frac{T}{\tau} \right) \right], \quad (18)$$

where  $E(x, k)$  is the incomplete elliptic integral of the second kind. We note that the above expression from the DDP method approaches the exact analytical Landau-Zener formula,  $P \rightarrow e^{-\pi\Lambda/2}$ , as  $T \rightarrow \infty$ .

In the following, we address results for  $(T, \tau, \Lambda) = (2, 1, 1)$  (for which  $T > \tau$  is satisfied and the DDP method works) from a new method we propose by Eq. (15). In Fig. 2 we show the analytical structure of  $F(t)$  read from Eq. (16) with the steepest descents and ascents. We implicitly assume some scale  $t_0$  of  $t$  and measure  $T$  and  $\tau$  in units of  $t_0$  [where  $t_0$  finally goes away, see Eq. (18)]. In Fig. 2 the blue dotted line represents the DDP contour attached to the closing point  $t_c$  shown by the open-circle dots. It is clear that the poles shown by the cross dots are harmless for the DDP contour deformation in this case. Three filled-circle dots denote the saddle points  $t_s$  of  $F(t)$ . Solid and dashed lines represent the steepest descents and ascents, respectively. Only the upper (red) steepest ascent crosses the original integration contour (namely, the real axis), so that the upper (red) steepest descent has  $n = 1$  and contributes to recover the original integration. Two saddle points and one steepest descent (black solid line) in  $\text{Im } t < 0$  region are completely irrelevant since the associated Morse index is vanishing. We make a brief remark on

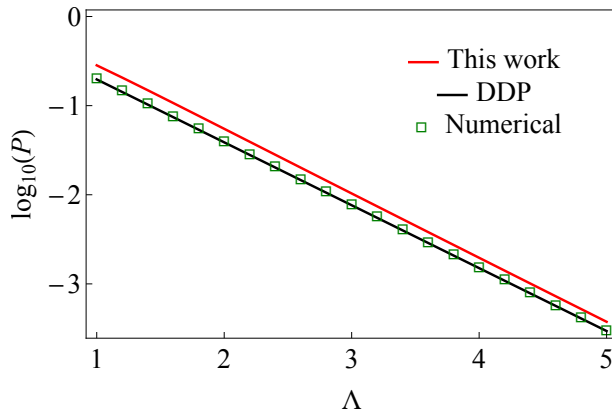


Figure 3: Comparison of  $P$  as a function of  $\Lambda$  in the modified Landau-Zener model with  $(T, \tau) = (2, 1)$ . The upper (and lower) solid line represents the results from this work (and the DDP method, respectively). The open-square dots represent the full numerical results without truncation.

branch cuts on Fig. 2. Our choice of branch cuts runs from  $t = \pm i\tau, \pm iT$  along the imaginary axis in such a way that they never cross the real axis.

For this case of  $(T, \tau) = (2, 1)$  Fig. 3 presents  $P$  as a function of  $\Lambda$ ; the red solid line represents the estimate from our new method, the black solid line shows the DDP results, and the green open-square dots are from the direct numerical calculation (without truncation).

One might think that the DDP method shows good agreement with numerical calculations. In fact such good agreement is quite unnatural and accidental; the DDP method relies on the first order truncation in the iterative approximation, while the numerical calculations shown here do *not*. Therefore, this level of agreement exceeds theoretical limitation. The point is that the DDP method artificially reproduces the exact analytical formula for the Landau-Zener model in the limit of  $T \rightarrow \infty$ , and so the deviation is still negligibly small even at  $T = 2$ . Thus, we must conclude that this too good agreement of the DDP method is due to a rather accidental reason.

In contrast, the Lefschetz-thimble inspired method is mathematically founded on the Picard-Lefschetz theory. We should emphasize that the results from our method in Fig. 3, especially the exponential slope, is reasonably consistent with the numerical calculations within approximation uncertainties. It is not very surprising that the exponents from the DDP method and ours are such close. Actually, the exponent is dominated by the contribution from  $\Delta(t)$ , and a shift from  $\eta(t)$  affects only the prefactor. On Fig. 2 we see that in  $\text{Im } t > 0$  region the open-circle dot ( $t_c$ ) and the filled-circle dot ( $t_s$ ) are located differently, and their spacing is given by the effect of  $\eta(t)$ . More interestingly, in Fig. 2, the blue dotted line denotes the DDP deformed contour [on which  $\text{Im } \Delta(t) = \text{Im } \Delta(t_c)$ ], and this is completely different from the red solid line of our contour [on which  $\text{Im } F(t) = (\text{const.})$ ]. According to our knowledge on the Picard-Lefschetz theory there is no strict reason why the blue dotted line of the DDP contour should be favored for the evaluation of Eq. (7).

### 2.3.2. When the DDP method fails

For  $T \leq \tau$  the DDP method is inapplicable due to the pole at  $t = iT$ , whereas our method is still operative. It is very interesting to see how our method circumvents the pole in complex- $t$  plane. In Fig. 4 we show the analytical structure of  $F(t)$  with the steepest descents and ascents



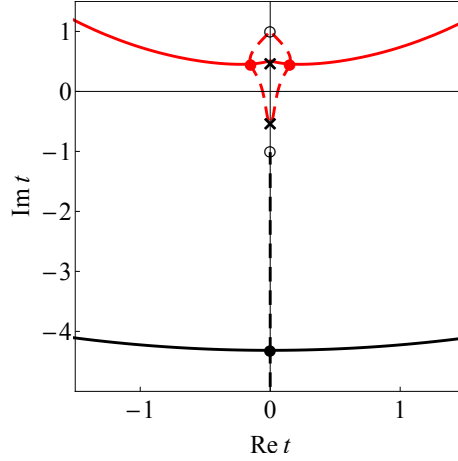


Figure 4: Analytical structure of  $F(t)$  in complex- $t$  plane in the modified Landau-Zener model with  $(T, \tau, \Lambda) = (\frac{1}{2}, 1, 1)$ . The upper (and lower) solid line represents the steepest descent with  $n = 1$  (and  $n = 0$ , respectively). The dashed lines are the steepest ascents. The cross dots represent the poles, the open-circle dots indicate the closing points, and the filled-circle dots are the saddle points.

for  $(T, \tau, \Lambda) = (\frac{1}{2}, 1, 1)$ , for which  $T < \tau$  and the DDP method does not work. Two filled-circle dots of the saddle points in  $\text{Im } t > 0$  region have the steepest ascents crossing the real axis, and so the associated steepest descents contribute to the integral, i.e.,  $n = 1$ . As mentioned before, we choose branch cuts along the imaginary axis to avoid crossing the real axis. In Fig. 4, strictly speaking, the black saddle point on the branch cut is degenerated, but such an analytical structure is irrelevant, for these saddle points make no contribution in our approach (i.e., the associated  $n = 0$ ). Here, the contour modifications induced by  $\eta(t)$  play an important role to avoid the pole. As mentioned before, the open-circle dots are changed to the filled-circle dots due to  $\eta(t)$ . In Fig. 4 we notice that two thimbles appear associated with two saddle points, and one edge of each is attached to the pole. Thus, the pole is not crossed over, so that the original integral is recovered exactly. Such analytical structures hold for general  $T < \tau$ .

Figure 5 presents  $P$  for  $(T, \tau) = (\frac{1}{2}, 1)$  as a function of  $\Lambda$ ; the red solid line represents the estimate from our new method and the green open-square dots are from the full numerical calculation. There is no data from the DDP method that simply does not work. We see a sharp suppression of the probability around  $\Lambda \simeq 10$ . This singular behavior is understandable from the similarity between the modified Landau-Zener and the Rosen-Zener models [49]. Our present work agrees fairly well with the numerical calculation except for the region in the vicinity of  $\Lambda \simeq 10$ . One possible explanation for this discrepancy around  $\Lambda \simeq 10$  lies in the first order truncation approximation to set  $a_-(t) = 1$  when we derived Eq. (7). In the region where  $P$  is vanishingly small, higher order terms from multiple transitions between  $|\chi_{\pm}(t)\rangle$  are no longer negligible.

Now, we put our emphasis on the robustness of our new method compared with the DDP method. The probability,  $P(\tau, T; \Lambda)$ , is a function of  $T$ ,  $\tau$ , and  $\Lambda$ . We could have shown a 3D plot of  $P(\tau, T; \Lambda)$  for a fixed  $\Lambda$  but, here, we plot  $P(\tau, 3 - \tau; 10)$  as a function of  $\tau$  as shown in Fig. 6. This is a 2D cross section of  $P(\tau, T; 10)$  cut by  $T = 3 - \tau$  along which we can see both regions where the DDP method does and does not work. For  $\tau \geq 1.5$  the DDP method is inoperative, on

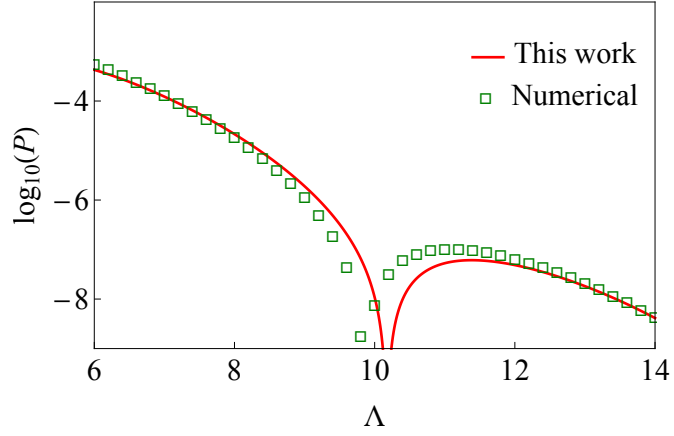


Figure 5: Comparison of  $P$  as a function of  $\Lambda$  in the modified Landau-Zener model with  $(T, \tau) = (\frac{1}{2}, 1)$ . The solid line represents the results from this work and the open-square dots represent the numerical results.

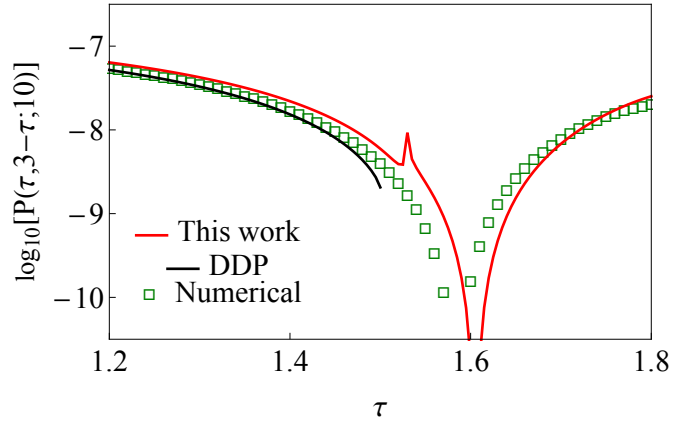


Figure 6: 2D cross section of  $P(\tau, T; \Lambda = 10)$  cut at  $T = 3 - \tau$ . The upper (and lower) solid line represents the results from this work (and the DDP method, respectively). The open-square dots represent the numerical results.

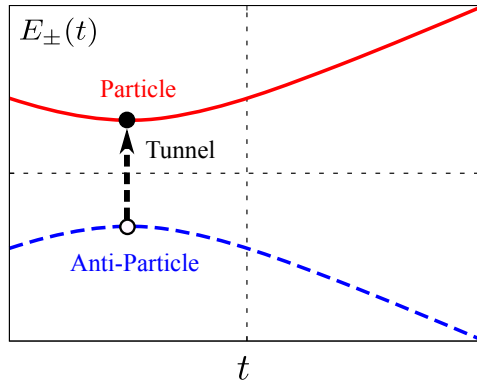


Figure 7: Particle and anti-particle energy levels for a constant electric field. The pair production process corresponding to quantum tunneling from the anti-particle to the particle state.

the one hand, so the black line ends at  $\tau = 1.5$  in Fig. 6. Our method, on the other hand, gives consistent estimates for any  $\tau$ , including the parameter region of  $[(T, \tau, \Lambda)|T \leq \tau]$  which the DDP method fails to access.

Let us make a couple of comments on Fig. 6. Firstly, we notice a peak around  $\tau \approx 1.55$  in this work. This peak is caused by the fact that the structure of the steepest descents drastically changes at  $\tau \approx 1.55$ . In fact, the analytical structure changes from one like Fig. 2 to the other like Fig. 4. Accordingly one critical point that contributes to the integral splits into two. These two critical points are close to each other shortly after the splitting, so the Gaussian approximation, as done in Eq. (15), becomes unreliable around  $\tau \approx 1.55$ . Secondly, we again see a sharp suppression of the probability around  $\tau \approx 1.6$ , as in Fig. 5. The underlying mechanism for this suppression is identical with the previous discussions. Overall, we can conclude that our new method supersedes the DDP method.

### 3. Schwinger Mechanism

As another interesting application let us discuss the Schwinger Mechanism. One might have an impression that the pair production problem in Quantum Field Theories appears to be distinct from two-level quantum mechanical problems. As correctly pointed out by Cohen and McGady [48], however, the Dirac equation for the Schwinger Mechanism reduces to the same form as the Landau-Zener model. We can immediately make sure that the exponential factor well known for the Schwinger Mechanism is readily derived from the DDP method, as sketched below. Then, a further challenging question is when the DDP method breaks down and how our method finds the correct answer.

#### 3.1. Constant electric field

The pair production process is nothing but a transition from the anti-particle state (with negative energy) to the particle state (with positive energy) as sketched in Fig. 7. In this paper we limit ourselves to systems with translational invariance. Then, the spatial momenta are simply labels for eigenenergies and there will be no mixing. More specifically, if the external electric

field is spatially homogeneous and along the  $z$  axis, the system is effectively described by the following Hamiltonian;

$$H(t) = \begin{bmatrix} p_z - eA_z(t) & m_\perp \\ m_\perp & -p_z + eA_z(t) \end{bmatrix}, \quad (19)$$

where we introduced  $m_\perp = \sqrt{p_x^2 + p_y^2 + m^2}$ . This form of the Hamiltonian corresponds to the Landau-Zener model with  $\alpha(t)$  and  $V(t)$  in Eq. (1) chosen as

$$\alpha(t) = 2[p_z - eA_z(t)], \quad V(t) = 2m_\perp. \quad (20)$$

In the case of the constant electric field,  $A_z(t) = -Et$ , two adiabatic eigenenergies, namely, two eigenvalues of the matrix (19) are

$$E_\pm(t) = \pm \sqrt{(p_z + eEt)^2 + m_\perp^2}. \quad (21)$$

We can also calculate the adiabatic factor,  $\eta(t)$ , which plays a pivotal role in our method. For this problem, obviously, there is no pole in  $\delta E(t)$  and the DDP method works. We assume below that the mass gap is larger than the magnitude of the electric field,  $m^2 \gg eE$ .

The particle and the anti-particle levels do not touch as long as  $t$  is real, as is obvious in Fig. 7. In the complex- $t$  plane we can locate the closing point simply from the condition,  $E_\pm(t = t_c) = 0$ , from which we find,

$$t_c = -\frac{p_z}{eE} + i\frac{m_\perp}{eE}. \quad (22)$$

We can say that the classically prohibited Schwinger process becomes possible for  $t$  to take such a detour to  $t_c$  where two states touch. According to Eq. (10) we can immediately find the exponent as

$$\begin{aligned} -2\text{Im} \Delta(t_c) &= -4\text{Im} \int_0^{t_c} dt \sqrt{(p_z + eEt)^2 + m_\perp^2} \\ &= -\frac{2}{eE} \text{Im} \left\{ (p_z + eEt) \sqrt{(p_z + eEt)^2 + m_\perp^2} + m_\perp^2 \ln \left[ (p_z + eEt) + \sqrt{(p_z + eEt)^2 + m_\perp^2} \right] \right\}_{t=0}^{t=t_c} \\ &= -\frac{2m_\perp^2}{eE} \text{Im}[\ln(i)] = -\frac{\pi m_\perp^2}{eE}. \end{aligned} \quad (23)$$

Thus, we can approximate the transition probability,  $P \simeq e^{-\pi m_\perp^2 / (eE)}$ , as is perfectly consistent with the well-known Schwinger formula. We note that the prefactor for the (3+1)-dimensional theory should be retrieved from the transverse phase-space integration. This is a successful example to show how the DDP method is useful for a wide class of physics problems even in Quantum Field Theories.

### 3.2. Pulse electric field

A less successful example of the DDP formula application is soon encountered once the electric field profile gets time dependent. The analytical properties of the Sauter-type potential are well understood (see Ref. [12] and references therein), which is given by

$$eA_z(t) = -\frac{eE}{\omega} \tanh(\omega t), \quad (24)$$

leading to a pulse-shaped profile of electric field, i.e.,

$$eE(t) = \frac{eE}{\cosh^2(\omega t)}. \quad (25)$$

Now, for later convenience, let us introduce the Keldysh adiabaticity parameter as done in Ref. [38] as

$$\gamma = \frac{m\omega}{eE}. \quad (26)$$

The electric profile smoothly reduces to a constant electric field in the limit of  $\omega \rightarrow 0$  or  $\gamma \rightarrow 0$ . The Hamiltonian describing this system is Eq. (19) with Eq. (24). The energy difference in this case is,

$$\delta E(t) = 2 \sqrt{\left[ p_z + \frac{m}{\gamma} \tanh(\omega t) \right]^2 + m_\perp^2}. \quad (27)$$

The adiabatic factor,  $\eta(t)$ , is calculable straightforwardly as well. We again emphasize the importance of  $\eta(t)$  in comparing between the DDP method and our method. The closing points are located at

$$t_c = \frac{1}{\omega} \tanh^{-1} \left( -\frac{\gamma p_z}{m} + i \frac{\gamma m_\perp}{m} \right) + i \frac{2\pi k_1}{\omega} \quad (28)$$

for  $k_1 \in \mathbb{Z}$ . Because contributions from  $k_1 \neq 0$  are suppressed by large exponents, it would be sufficient for us to consider only the  $k_1 = 0$  contribution. For this specific choice of the vector potential, there are poles at

$$t_{\text{pole}} = i \frac{\pi(1 + 2k_2)}{2\omega} \quad (29)$$

with  $k_2 \in \mathbb{Z}$ . Now, let us assume a sufficiently small value of  $\omega$  so that  $\text{Im } t_{\text{pole}} \ll \text{Im } t_c$  and thus the DDP method definitely works. Under this condition the DDP method gives us an approximated expression,  $P \simeq e^{-Am^2/(eE)}$ , with

$$A = \frac{\pi}{\gamma m} \left[ \sqrt{\left( \frac{m}{\gamma} + p_z \right)^2 + m_\perp^2} + \sqrt{\left( \frac{m}{\gamma} - p_z \right)^2 + m_\perp^2} - \frac{2m}{\gamma} \right], \quad (30)$$

which can be further simplified into

$$A \simeq \frac{\pi m_\perp^2}{2m} \left( \frac{1}{m + \gamma p_z} + \frac{1}{m - \gamma p_z} \right) \quad (31)$$

for  $\gamma(p_z/m) \ll 1$ . This exactly agrees with the expanded results from the analytical answer [50]. Clearly, we recover the previous result for constant electric field in the adiabatic  $\gamma \rightarrow 0$  limit. It is also natural that  $A \rightarrow \infty$  and thus  $P \rightarrow 0$  as  $p_z$  approaches  $\pm m/\gamma = \pm eE/\omega$  since the maximum  $p_z$  should be an impulse by a force  $eE$  and a duration  $1/\omega$ . If  $p_z$  exceeds this maximum, the pair production is disfavored and  $P \rightarrow 0$  follows.

In the opposite limit of  $\gamma \gg 1$  the impulse approximation would work better to justify the perturbative expansion. However, from Eq. (30),  $A \rightarrow 0$  and  $P \rightarrow 1$  is concluded in the  $\gamma \rightarrow \infty$  limit. In this case the DDP method does not give the correct asymptotic behavior. The reason why the DDP method does not work is more nontrivial than the modified Landau-Zener model. In fact, with the Sauter-type electric field, the DDP contour is deformable without hitting any pole in the complex- $t$  plane. The validity lost of the DDP method is attributed to the adiabatic factor  $\eta(t)$

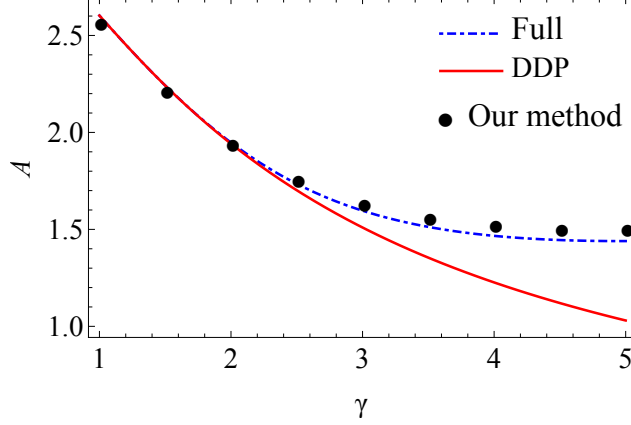


Figure 8: Comparison of  $A$  of  $P \simeq e^{-Am^2/(eE)}$  as a function of the Keldysh parameter  $\gamma$  between the full answer (dotted line), the DDP method (solid line), and our estimates (filled circles) for  $m = 3$  and  $eE = 3$  at  $\mathbf{p} = 0$  in arbitrary unit.

which is not taken into account in the determination of  $t_c$ . Our results from the Lefschetz-thimble inspired method take care of  $\eta(t)$ , so that they can be consistent with the full answer.

Figure 8 presents a quantitative comparison between the full answer (dotted line), the DDP method (solid line), and our estimates (filled circles). The DDP method is a pretty good approximation for  $\gamma \lesssim 2$ , but it loses the agreement with the full answer for larger  $\gamma$ . In contrast, owing to the inclusion of  $\eta(t)$ , our method gives reasonably approximating results for overall  $\gamma$ .

### 3.3. Dynamically Assisted Schwinger Mechanism

Finally, let us consider an example which has attracted a lot of theoretical attentions. That is, we will consider a combination of a constant electric field and a pulsed one, which is represented by the following vector potential,

$$eA_z(t) = -eEt - \frac{e\varepsilon}{\omega} \tanh(\omega t), \quad (32)$$

where  $\varepsilon/E \ll 1$  is presumed. In the same way as the previous subsection, we can immediately obtain the adiabatic energy difference,

$$\delta E(t) = 2 \sqrt{\left[ p_z + eEt + \frac{e\varepsilon}{\omega} \tanh(\omega t) \right]^2 + m_\perp^2}. \quad (33)$$

The cloing points are the solutions of

$$\omega t_c + \frac{\varepsilon}{E} \tanh(\omega t_c) = -\frac{\gamma p_z}{m} + i \frac{\gamma m_\perp}{m}. \quad (34)$$

Here, we should note that we share the same notation,  $\gamma$ , as defined in Eq. (26), but the meaning of  $E$  and  $\omega$  in this subsection are different from the previous subsection;  $\omega$  is a frequency of the field whose strength is not  $E$  but  $\varepsilon$  now. The pair production at  $\mathbf{p} = 0$  has the least exponential suppression, so we set  $\mathbf{p} = 0$  for simplicity below. This choice simplifies the location of the

closing points and enables us to perform analytic calculation to some extent. The closing points,  $t_c = i\tau_c$ , are the solutions of

$$\omega\tau_c + \frac{\varepsilon}{E} \tan(\omega\tau_c) = \gamma. \quad (35)$$

Although  $\varepsilon/E \ll 1$ , the second term in the left-hand side of Eq. (35) is not negligible because of the singularities from  $\tan(\omega\tau_c)$ . The above singularities also give the poles of  $\delta E(t)$ , i.e.,

$$t_{\text{pole}} = i \frac{\pi(1+2k)}{2\omega} \quad (36)$$

with  $k \in \mathbb{Z}$  just in the same manner as in Eq. (29).

The solutions of Eq. (35) can be easily drawn by the crossing points between two functions,  $(\varepsilon/E) \tan(x)$  and  $-x + \gamma$ , where  $x = \omega\tau_c$ . Because of the divergent behavior of  $\tan(x)$ , the closing point nearest to the origin in the upper complex- $t$  plane is  $\omega\tau_c = \pi/2 - \delta$  ( $\delta \ll 1$ ) for  $\gamma \gtrsim \pi/2$ . Therefore, for sufficiently small  $\gamma \ll 1$ , we see that  $t_{\text{pole}}$  does not intrude the region of the contour deformation toward  $t_c = i\tau_c$ , and the DDP method should work. Indeed, the DDP method gives us the asymptotic form of the probability,  $P \simeq e^{-Am^2/(eE)}$ , with

$$A = \frac{2\pi}{\gamma} \quad (37)$$

for  $\gamma \gg 1$ . This asymptotic behavior inferred from the DDP formula agrees with the result from the worldline instanton [38]. It should be noted that the direct comparison is little subtle; we computed the rate for  $\mathbf{p} = 0$  for simplicity, and the exponent (or the vacuum decay probability) obtained in Ref. [38] is a quantity after the whole phase-space integration. As long as we focus on the exponent only, the quantitative comparison still makes sense since the  $\mathbf{p} = 0$  contribution is dominant.

When we derived the asymptotic form of the DDP formula, we only imposed  $\gamma \gg 1$  and  $E \gg \varepsilon$ . However, another condition,  $m \gg \omega$ , is required to justify the worldline instanton calculus in order to prohibit the dynamical pair production. Figure. 9 presents a detailed comparison between the full answer (dot-dashed line), the DDP method (solid line), the worldline method (dotted line), and our estimate (filled circles) when we chose  $m = 3$ ,  $eE = 3$  and  $\varepsilon = 0.3$ . We can confirm that the DDP and the worldline results approach each other for large  $\gamma$ , as is consistent with the analytical consideration. A surprise comes from the fact that the full answer from the brute-force numerical calculation deviates from the DDP and the worldline results, which is to be explained by the breakdown of  $m \gg \omega$  for large  $\gamma$  with the current parameter set. Our results from the Lefschetz-thimble inspired method tend to stay closer to the full answer than the other methods. The improvement is again ascribed to the adiabatic factor  $\eta(t)$  which is taken into account in our method.

#### 4. Conclusions

We studied the Dykhne-Davis-Pechukas (DDP) method to describe a transition amplitude in two-level quantum systems and proposed an alternative method inspired by the Lefschetz-thimble method. Since the DDP method is based on complex deformation of the time integration, one may think that the DDP method is justified directly from the complex analysis. Contrary to that, however, the one dimensional application of the Picard-Lefschetz theory implies that the optimal contour is different from the one adopted in the DDP method.

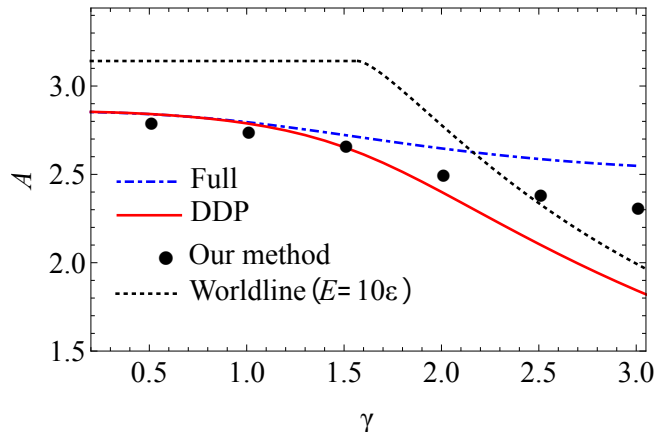


Figure 9: Comparison of  $A$  of  $P \simeq e^{-Am^2/(eE)}$  as a function of the Keldysh parameter  $\gamma$  between the full solution (dotted line), the DDP method (solid line), and our estimates (filled circles) for  $m = 3$ ,  $eE = 3$ , and  $\varepsilon = 0.3$  at  $p = 0$  in arbitrary unit.

With some parameters of the Hamiltonian for which the DDP complex- $t$  contour goes across poles and/or the closing points are too close to poles, the DDP method breaks down. Our proposed method can evade this problem thanks to the pole-free structure of the steepest descents whose shape is affected by poles. We explicitly tested the performance of our method in the modified Landau-Zener model. The comparison between the direct numerical calculation, the DDP method, and our method confirmed that our method can give a reasonable approximation for all parameter regions even when the DDP method cannot.

Two-level quantum systems include interesting modeling of quantum field-theoretical problems. Among them, we treated the Schwinger Mechanism, i.e., the pair production of a particle and an anti-particle under electric fields, as a two-level quantum problem in the Landau-Zener model. For the constant electric field the DDP method gave an answer fully consistent with the known formula. We found, however, that the approximation of the DDP method gets worse for pulsed shapes of electric fields if the pulse is short-lived and the adiabatic factor is not negligible for large Keldysh factor  $\gamma > 2$ . In contrast our method gives results in agreement with the full numerical answer for parameters when the DDP method loses validity. We further applied these methods for the Dynamically Assisted Schwinger Mechanism in which the exponential threshold is suppressed. Our calculations show that both the DDP method and our method match well with the full answer for small  $\gamma$  regions. The interesting is for larger  $\gamma > 2$  where the DDP method ceases working well. The DDP method leads to an exponent that asymptotically approaches the value obtained in the worldline instanton method as  $\gamma \rightarrow \infty$  (in which the worldline instanton calculus is anyway out of validity region). In our method the adiabatic factor is taken into account and the approximated estimate turns out to be closer to the full answer than other methods.

There are various future directions to extend the current work. One of them lies in a closer look at the foundation of the DDP method. The Picard-Lefschetz theory cannot justify the DDP method, but it is certainly true that the DDP method somehow reproduces the exact analytical results for the Landau-Zener model and there might be some underlying mechanisms for such a coincidence. Besides, as we found, the DDP method seems to be compatible with the worldline instanton method, and its reasoning would be, if any, quite interesting to seek for.



Finally, we shall mention an intriguing possibility for future works. In addition to advantages in a sense of adaptivity of our method, it could be the case that our method can be a new tool to reveal some drastic changes of model features like a phase transition. It is actually known that the structure of the steepest descents or the Lefschetz thimbles in more general may suddenly change, which is referred to as the Stokes phenomenon. In the examples taken in this work, there was not such drastic and sudden alteration in the structure of the steepest descents, but if we consider a wider class of physics problems such as the Floquet-type problems with time periodic electric disturbances, some transitional changes would be caused. Once the Stokes phenomenon is involved, our method would be far superior to other methods. Our new method awaits phenomenological applications in the band theory of solids as well as in quantum field-theoretical problems such as the Schwinger Mechanism with more general time-dependent electric/magnetic profiles, the Hawking radiation on top of various metrics for which the analytical Bogoliubov coefficients are not calculable, etc, which will be reported elsewhere.

### acknowledgments

The authors thank Takashi Oka and Kazuaki Takasan for stimulating comments and discussions. This work was supported by Japan Society for the Promotion of Science (JSPS) KAKENHI Grant No. 18H01211 and 19K21874.

### References

- [1] T. Oka and H. Aoki, *Phys. Rev. B* **81**, 033103 (2010).
- [2] T. Oka, *Phys. Rev. B* **86**, 075148 (2012).
- [3] M. V. Berry, *Journal of Physics A: Mathematical and Theoretical* **42**, 365303 (2009).
- [4] N. A. Sinitsyn, E. A. Yuzbashyan, V. Y. Chernyak, A. Patra, and C. Sun, *Phys. Rev. Lett.* **120**, 190402 (2018).
- [5] G. S. Vasilev, A. Kuhn, and N. V. Vitanov, *Phys. Rev. A* **80**, 013417 (2009).
- [6] S. Guérin, V. Hakobyan, and H. R. Jauslin, *Phys. Rev. A* **84**, 013423 (2011).
- [7] H. Zhang, X.-K. Song, Q. Ai, H. Wang, G.-J. Yang, and F.-G. Deng, *Opt. Express* **27**, 7384 (2019).
- [8] R.-Q. Ma, B.-Y. Chai, M. Liang, Z.-L. Duan, W.-W. Zhang, J. Dong, and J. Shi, *Optics Communications* **430**, 1 (2019).
- [9] F. Sauter, *Z. Phys.* **69**, 742 (1931).
- [10] W. Heisenberg and H. Euler, *Z. Phys.* **98**, 714 (1936), arXiv:physics/0605038 [physics] .
- [11] J. S. Schwinger, *Phys. Rev.* **82**, 664 (1951).
- [12] G. V. Dunne, in *From fields to strings: Circumnavigating theoretical physics. Ian Kogan memorial collection (3 volume set)*, edited by M. Shifman, A. Vainshtein, and J. Wheeler (2004) pp. 445–522, arXiv:hep-th/0406216 [hep-th] .
- [13] F. Gelis and N. Tanji, *Prog. Part. Nucl. Phys.* **87**, 1 (2016), arXiv:1510.05451 [hep-ph] .
- [14] M. K. Parikh and F. Wilczek, *Phys. Rev. Lett.* **85**, 5042 (2000), arXiv:hep-th/9907001 [hep-th] .
- [15] L. D. Landau, *Z. Sowjetunion* **2**, 46 (1932).
- [16] C. Zener and R. H. Fowler, *Proceedings of the Royal Society of London. Series A, Containing Papers of a Mathematical and Physical Character* **137**, 696 (1932).
- [17] A. Dykhne, *Sov. Phys. JETP* **14**, 1 (1962).
- [18] J. P. Davis and P. Pechukas, *The Journal of Chemical Physics* **64**, 3129 (1976).
- [19] K.-A. Suominen, B. Garraway, and S. Stenholm, *Optics Communications* **82**, 260 (1991).
- [20] N. V. Vitanov and K.-A. Suominen, *Phys. Rev. A* **59**, 4580 (1999).
- [21] M. Wilkinson and M. A. Morgan, *Phys. Rev. A* **61**, 062104 (2000).
- [22] T. A. Laine and S. Stenholm, *Phys. Rev. A* **53**, 2501 (1996).
- [23] N. Vitanov and S. Stenholm, *Optics Communications* **127**, 215 (1996).
- [24] E. Witten, (2010), arXiv:1009.6032 [hep-th] .
- [25] E. Witten, *Chern-Simons gauge theory: 20 years after. Proceedings, Workshop, Bonn, Germany, August 3-7, 2009*, AMS/IP Stud. Adv. Math. **50**, 347 (2011), arXiv:1001.2933 [hep-th] .

- [26] M. Cristoforetti, F. Di Renzo, and L. Scorzato (AuroraScience), *Phys. Rev.* **D86**, 074506 (2012), arXiv:1205.3996 [hep-lat] .
- [27] M. Cristoforetti, F. Di Renzo, A. Mukherjee, and L. Scorzato, *Phys. Rev.* **D88**, 051501 (2013), arXiv:1303.7204 [hep-lat] .
- [28] H. Fujii, D. Honda, M. Kato, Y. Kikukawa, S. Komatsu, and T. Sano, *JHEP* **10**, 147 (2013), arXiv:1309.4371 [hep-lat] .
- [29] Y. Tanizaki, Y. Hidaka, and T. Hayata, *New J. Phys.* **18**, 033002 (2016), arXiv:1509.07146 [hep-th] .
- [30] Y. Tanizaki and T. Koike, *Annals Phys.* **351**, 250 (2014), arXiv:1406.2386 [math-ph] .
- [31] A. Cherman and M. Unsal, (2014), arXiv:1408.0012 [hep-th] .
- [32] A. Andreassen, D. Farhi, W. Frost, and M. D. Schwartz, *Phys. Rev.* **D95**, 085011 (2017), arXiv:1604.06090 [hep-th] .
- [33] A. Behtash, G. V. Dunne, T. Schaefer, T. Sulejmanpasic, and M. Unsal, *Annals of Mathematical Sciences and Applications* **Volume 2**, No. 1 (2017), arXiv:1510.03435 [hep-th] .
- [34] O. Gould and A. Rajantie, *Phys. Rev.* **D96**, 076002 (2017), arXiv:1704.04801 [hep-th] .
- [35] P. Draper, *Phys. Rev.* **D98**, 125014 (2018), arXiv:1809.10768 [hep-th] .
- [36] O. Gould, S. Mangles, A. Rajantie, S. Rose, and C. Xie, *Phys. Rev.* **A99**, 052120 (2019), arXiv:1812.04089 [hep-ph] .
- [37] O. Gould, A. Rajantie, and C. Xie, *Phys. Rev.* **D98**, 056022 (2018), arXiv:1806.02665 [hep-th] .
- [38] R. Schutzhold, H. Gies, and G. Dunne, *Phys. Rev. Lett.* **101**, 130404 (2008), arXiv:0807.0754 [hep-th] .
- [39] G. V. Dunne, H. Gies, and R. Schutzhold, *Phys. Rev.* **D80**, 111301 (2009), arXiv:0908.0948 [hep-ph] .
- [40] M. Orthaber, F. Hebenstreit, and R. Alkofer, *Phys. Lett.* **B698**, 80 (2011), arXiv:1102.2182 [hep-ph] .
- [41] C. Fey and R. Schutzhold, *Phys. Rev.* **D85**, 025004 (2012), arXiv:1110.5499 [hep-th] .
- [42] Z. L. Li, D. Lu, B. S. Xie, L. B. Fu, J. Liu, and B. F. Shen, *Phys. Rev.* **D89**, 093011 (2014).
- [43] P. Copinger and K. Fukushima, *Phys. Rev. Lett.* **117**, 081603 (2016), [Erratum: *Phys. Rev. Lett.* 118, no.9,099903(2017)], arXiv:1605.05957 [hep-th] .
- [44] C. Schneider and R. Schutzhold, *Phys. Rev.* **D94**, 085015 (2016), arXiv:1603.00864 [hep-th] .
- [45] G. Torggrimsson, C. Schneider, J. Oertel, and R. Schutzhold, *JHEP* **06**, 043 (2017), arXiv:1703.09203 [hep-th] .
- [46] G. Torggrimsson, C. Schneider, and R. Schutzhold, *Phys. Rev.* **D97**, 096004 (2018), arXiv:1712.08613 [hep-ph] .
- [47] M. V. Berry, *Proceedings of the Royal Society of London. A. Mathematical and Physical Sciences* **429**, 61 (1990).
- [48] T. D. Cohen and D. A. McGady, *Phys. Rev.* **D78**, 036008 (2008), arXiv:0807.1117 [hep-ph] .
- [49] N. Rosen and C. Zener, *Phys. Rev.* **40**, 502 (1932).
- [50] K. Fukushima, F. Gelis, and T. Lappi, *Nucl. Phys.* **A831**, 184 (2009), arXiv:0907.4793 [hep-ph] .